ISSN: 2639-7455

Research Article

Earth & Environmental Science Research & Reviews

Geophysical Based Groundwater Potential Zone Mapping: Perspectives and Inferences from Lisana Area along the Guder River, Western Margin of the Central Main Ethiopian Rift

Esubalew Yehualaw[1,2] and Tigistu Haile[1]

[1]*School of Earth Sciences, Addis Ababa University, Addis Ababa, Ethiopia*

[2]*Ethiopian Ministry of Mines, Department of Petroleum and Geothermal, P.O Box 486, Ethiopia, Addis Ababa*

***Corresponding Author**

Esubalew Yehualaw, School of Earth Sciences, Addis Ababa University, Addis Ababa, Ethiopia.

Submitted: 2023, Aug 02; **Accepted**: 2023 Sep 15; **Published**: 2023 Sep 25

Citation: Yehualaw, E., Haile, T. (2023). Geophysical based groundwater potential zone mapping: Perspectives and inferences from Gode area, western margin of the Central Main Ethiopian Rift. *Earth Envi Scie Res & Rev, 6*(4), 604-615.

Abstract

Vertical electrical soundings and magnetic data were used to map the groundwater aquifer system in the Lisana area along the Guder River, northeast of Hosanna town, near the western margin of the Central Main Ethiopian Rift. The surveys were used to map a potential aquifer zone and investigate the groundwater potential for the current and future development of the resource in the Lisana area. The VES data were used to map the depth of a potential aquifer zone and its distribution over the area. The magnetic survey was used to delineate contacts between lithologic units and geological structures. Two-dimensional magnetic forward modeling and one-dimensional electrical modeling were used to identify fractures and lithological units containing potential groundwater. The magnetic and electrical resistivity modeling indicated that a potential aquifer occurs at a depth range from 115m to 142m. The potential aquifer occurs within weathered and fractured ignimbrite and a pumice layer containing sandy soil. This latter lithological unit is the main water-bearing horizon.

Keywords: Vertical Electrical Soundings, Magnetics, Aquifer, Groundwater Potential, Ethiopia

1. Introduction

Water is a basic component of life and central to all efforts to address food security, economic growth, and energy production [1]. With time, due to population growth and the expansion of irrigation activity, the use and sustainability of water resources have become scarce [2]. Therefore, it is of great importance that water resources of an area should be located, developed, and used sustainably to maintain an adequate water supply and preserve the environment for the availability of groundwater resources.

Groundwater is an essential resource, and it is a crucial source of freshwater worldwide [3]. Showed that the occurrence and distribution of groundwater aquifers in Ethiopia depend on several environmental and geological factors. Amongst the geological factors, the variation in rock type is most important as the groundwater potential varies sometimes within a few meters and even within the same geological formation [4].

Geological and geophysical investigations have been increasingly used to study the lithological, hydraulic, and petrophysical characteristics of the different portions of aquifer systems in Africa and Ethiopia in particular [5-10]. Surface geological and borehole, while important, cannot determine the detailed three-dimensional subsurface characteristics of an aquifer system and thus, geophysical methods (seismic, electrical resistivity, electromagnetics, and magnetics) offer a significant advantage for groundwater resource mapping and water quality evaluation. With the increase available of sophisticated but relatively easy-to-use geophysical equipment and modeling software, the use of geophysical investigations has increased dramatically over the last decades [11].

In the southernmost regions of Ethiopia, especially in Hadiya Zone shown by the irregular yellow solid line (Fig. 1), groundwater is important for domestic, agricultural, and industrial uses [9]. However, the Hadiya Zone (Fig. 1), has frequently been affected by recurrent droughts, and as a result, the population does not have a secure food source, especially in the study area. Hosanna and the surrounding region are currently obtaining their water supply from boreholes and springs found near the Guder River within the study area (Fig. 1). Even though these boreholes are drilled near the Guder River, besides from a study area (Fig. 3), there have been no geophysical investigations to determine the groundwater potential of the region surrounding the Guder River [9]. Additionally, some

of the existing boreholes are currently non-functional making the water scarcity even more acute [9]. Thus, the exploration of groundwater has not been adequate to solve the problems of the demand for clean water that is continuously raised in society.

The need for additional water sources in Hosanna and the surrounding rural areas is increasing due to population growth and the expansion of irrigation for agriculture. Identifying the potential and extent of the aquifer system in the Lisana area (Figure 2a) along the Guder River is necessary to satisfy the demand for clean water as well as to minimize the risk of drilling dry boreholes at inappropriate locations. To determine the potential and extent of the aquifer system, a geophysical study was undertaken using vertical electrical soundings (VES) and a magnetic survey. The VES data will be modeled by one-dimensional inversion methods and the magnetic data will be analyzed by derivative methods and two-dimensional modeling. The models will be used to determine the extent of the aquifer (VES) and any geological structures controlling the groundwater flow (magnetics).

2. Geology and Hydrogeology of The Study Area

2.1. The Study area

Hosanna is a part of the Southern Nation Nationalities and the People's Regional State (SNNPRS) of Ethiopia. It is situated within the Hadiya Zone (Fig. 1) and is located 230 km southwest of the capital of Ethiopia, Addis Ababa. Hosanna is located at the western margin of the Main Ethiopian Rift (MER). The study area of Lisana (Figure 2a), is located at about 8.4 km northeast of Hosanna (Fig. 1).

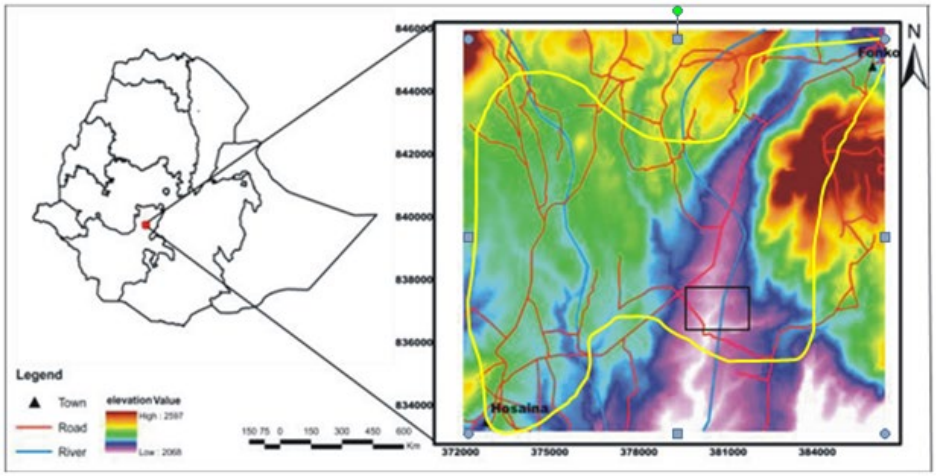

Figure 1: Location map of the study area where the left figure shows the location of the study area (red triangle) on the administrative map of Ethiopia. The right panel shows the physiography of the study area (black rectangle) and the surrounding region in the Hadiya zone shown by the irregular yellow solid line (Yehualaw et al., 2023).

2.2. Geology

The MER is a magmatic rift that has all stages of rift evolution from rift initiation to break up and incipient oceanic spreading [12]. It contains Cenozoic volcanic rocks and Tertiary and Quaternary sediments except for widely spaced Proterozoic outcrops [13]. (Figure 2a). Showed that the MER is divided geographically into three sectors: northern, central, and southern MER based on the style of deformation and amount and type of volcanism. The study area is in the Central Main Ethiopian Rift (CMER). The study area is covered by soils, except at river valleys. The geological units within the study site are ignimbrite, pyroclastic ash tuff, volcanic ash, and residual soils with brief descriptions of these different units below:

Volcanic Tuff: a pyroclastic unit is exposed in the study area's eastern, western, and southern portions along river cut and road sections. It is characterized by a white color and a fine-grained texture. The tuff unit is relatively porous and usually formed by the compaction and cementation of volcanic ash (Fig. 2a).

Ignimbrite: The ignimbrite is a welded tuff and is exposed along the Guder River in the northern and southern portions of the study area. Ignimbrite deposits are characterized by poorly sorted aggregates of tuff and pumice. The weathered and highly fractured ignimbrite is found in the southwestern portion of the study area (Fig. 2b). It is intercalated with reddish clay soil and tuff in many parts of river exposure. The intercalation shows depositional series of pyroclastic materials. Pyroclastic ash tuff: The tuff is well-sorted and fine to medium-grained. This pyroclastic unit is exposed in the western and southern portions of the study area along river cuts and road sections. It is characterized by white color and fine-grained texture (Fig. 2c).

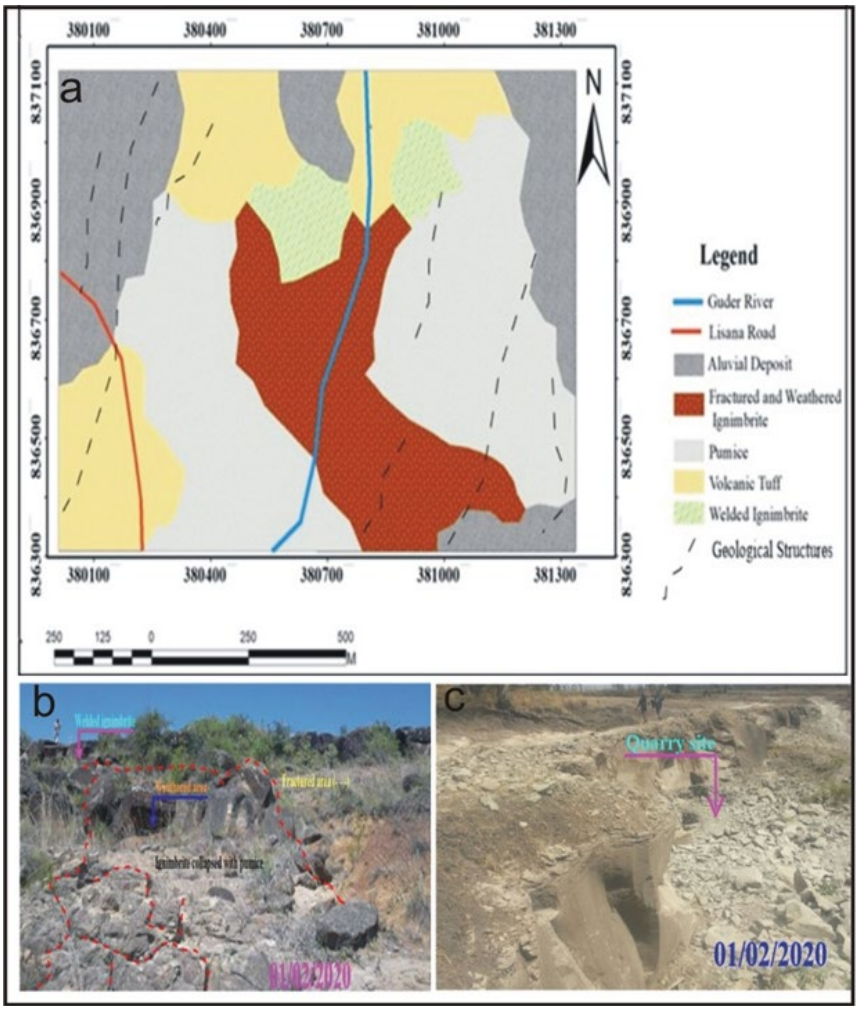

Figure 2: (a) Geological map of Gode area, (b) Photograph of the fractured and weathered ignimbrite with collapsed pumice layers within the southern part of the study area, and (c) Pyroclastic ash tuff and pumice at a quarry site (Yehualaw et al., 2023).

2.3. Hydrogeology of the study area

The hydrogeology is composed of aquifers and aquitards defined based on the character of the groundwater flow (pores and fissures), the yield of springs, and the hydraulic characteristics of boreholes. The central portion of the study area serves as the recharge area whereas the marginal portions are discharge areas. Various springs are found in the eastern, western, and southern portions of the study area. The main types of aquifers are discussed as follows:

2.3.1. Extensive and Moderately Porous and/or Fissure Aquifers

Quaternary volcanic rocks such as basalt and weathered and fractured ignimbrites have a fissured permeability and represent the porous aquifers of the area [9]. The western part of the study area has relatively high precipitation and is categorized with moderately productive aquifers [9].

2.3.2. Local and Moderately Productive Fissured Aquifer

Permeability is largely a function of rocks' porosity and structures (joints and fractures) where the welded ignimbrites usually alternate with non-welded ones and are intercalated with tuff, pumice, and lacustrine sediments. Some sections of Gode in the neighborhood of the study area have relatively low to moderate aquifers [9].

2.3.3. Formation Consisting of a Minor Fissured Aquifer-Aquitard

Aquitards are where groundwater is neither stored nor transmitted, with minimal water flow through these rocks. Due to some of the volcanic rocks being less fractured, these rocks act as aquitards in this region. Thus, it is difficult to get shallow wells in the northern region of the study area.

3. Materials and Methods

Electrical resistivity and magnetic surveys were used in this study for groundwater potential assessment and aquifer characterization in the Gode area to and along the Guder River (Fig. 3).

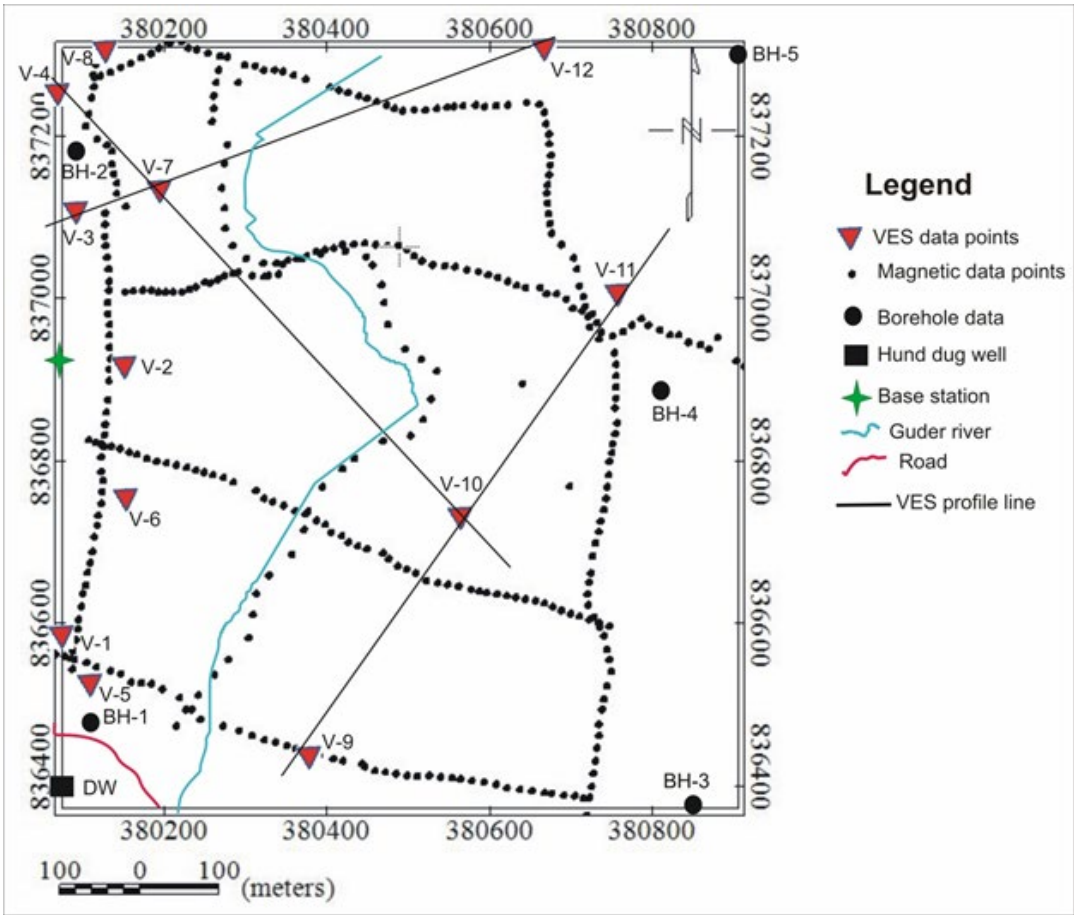

Figure 3. Location of the vertical electrical sounding and pseudo section profiles, magnetic data, and boreholes in the study area.

3.1. Electrical Resistivity

The Electrical resistivity method is one of the most important methods for groundwater investigation as it is one of the best methods in detecting groundwater content of subsurface lithologies and water quality [14-16]. The Schlumberger array [17, 18] is the most commonly used electrode array used in VES surveys. In the VES method, the positions of the current electrodes are changed concerning a fixed point and the electrical potentials reflect the distribution of resistivity values that vary with depth because of a vertical variation of electrical resistivities.

3.2. Magnetic Survey

A magnetic survey was conducted to demarcate the location of faults/ fractures that may govern the movement of groundwater. A proton precession magnetometer (GSM- 9T) was used to conduct the ground magnetic survey and Figure 4 shows the location of the data. During the the survey, all magnetic objects such as cars, power lines, metal pipes, and electrified railway lines were avoided to reduce data noise. More than 405 magnetic data were collected over two days, with the survey designed to commence during the morning hours to reduce the diurnal effects on the data. However, surveys were also taken in the late afternoon hours to optimize the field time available for the survey. The observations were made every 10 m over all transect lines of the VES and at 20 m station spacing for each random field distribution point. A base station was reoccupied within half-hour intervals to facilitate the correction of diurnal variation. The base station was located at UTM coordinates of an Easing of 380129 meters and a North of 836873 meters. The data acquisition always started and ended at the base station. The 2020 International Geomagnetic Reference Field (IGRF) was removed from the field data to create a residual magnetic anomaly data set.

4. Results and Discussion

4.1. VES analysis and aquifer characterization

VES data are commonly presented as depth-sounding curves, which can be obtained by plotting apparent resistivity values against electrode spacing on a log-log or bi-log graph paper. Raw field resistance data (in ohms) for all the VES point locations were converted to the apparent resistivity in (ohm-meter) by multiplying it with the appropriate geometric factor. Overall, error values of 1.9 - 4.7% were achieved. For this study, we show a representative VES station (VES-3) as an illustration of the graph (Fig. 4) and show the results of the one-dimensional inversion. The interpretation of VES-3 shows the possible subsurface lithologic units that are constrained using borehole BH-2 is also shown in (Figure 5). The final model (Figure 5) reveals four electrical resistivity layers of varying thickness and electrical resistivity

values and are interpreted as soil, soil with silt and clay, ignimbrite, and pumice from top to bottom respectively. The weathered layer (pumice) constitutes the hydrogeological significant layer because of its water-bearing capacity and is characterized by high porosity, relatively high permeability, and high specific yield [18].

4.2. Stacked and Iso-resistivity Maps

The stacked map of electrical resistivity values (Fig. 6a) was constructed using the one-dimensional resistivity models for AB/2=1.5, 20, 45, 220, 330, and 500m. Figure 8a shows the areas red solid and dashed lines outline high resistivity regions that may be barriers to groundwater flow and the white line shows the location of the Guder River. The Iso-resistivity plots (Fig. 5) show that in the northeast and southeastern portions of the plot that there is a low resistivity region that could be potential groundwater zones due to the increased thickness of the aquifer, especially in the region of VES-10 and VES- 11 (Fig. 5). Additionally, there is a relatively high resistivity zone in the southwest corner of the figure and around the central region. These areas may be aquitards.

4.3. Pseudo-Depth and Geoelectric Sections

Figures 5a, b, and c show pseudo-depth maps and the corresponding geoelectric layers compiled using all of the VES stations. Figure 5a shows three VES stations, VES-4, VES-7, and VES-10, and reveals that in the region between VES-4 and VES-7, close to VES-4, the subsurface is represented by the relatively low resistivity horizon. A similar property is observed beneath VES-10, showing a low resistivity region, at deeper and shallower depths. The above interpretations (especially at deeper depths) are indicative of potential water zones in the southeastern and northwestern parts of the study area (Fig. 5a).

The region beneath VES-10 is of interest from the point of view of this survey as the low resistivity values are recorded as a result of likely groundwater. Towards the NW along a projected line between VES- 10 and -11, the shallow subsurface appears to have a low resistivity and exhibits a gradual increase in resistivity with depth (Fig. 5b). The region under the section shows extensive coverage of the low resistivity zone between VES- 10 and VES- 11 (Fig. 5b). Figure 5c shows a distinct lateral variation in electrical resistivity with a prominent low resistivity in the top and bottom zones mapped around VES-3 and VES-12. A high resistivity zone is found in the region beneath VES-7, and some extend to VES-3. In the region beneath VES-3 and VES-12, the ground has a relatively low resistivity horizon and this low-resistivity region should be investigated for groundwater potential.

The geological sections in (Fig. 6) were constructed using the results of the one-dimensional modeling of the VES data and the lithology logs from nearby boreholes. A possible fault/fracture zone is depicted shown by the dashed solid line in Figures 5a, b, and c. A thin soil with varying electrical resistivities is due to the changing moisture content that is mapped as the first layer. The second layer corresponds to the moderately saturated ignimbrite layer. Underlying the top layer, beneath VES-9, the subsurface is characterized by high resistivities and has an average thickness of 20m. This layer is thought to be scoriaceous basalt with sand as correlated to the borehole log in the Gode area (Fig. 8). The potential fault/fracture zone, (Fig. 5a and b) may be a normal fault between VES-9 and VES-10 up to a depth of 25-182m, which may be a groundwater barrier. The third and fourth geoelectric horizons have a large lateral electrical resistivity variation concerning the layer beneath VES-10 and VES-11. The lowest portion of the sections is low to moderate resistivity with the response of highly weathered/ fractured pumice/ volcanic ash beneath VES-3, VES-4, VES-7, VES-9, VES-10, and VES-11(Figs. 5a, b, and c). This layer is interpreted as weathered/ fractured ignimbrite underneath all of the VES stations. The third layer's low resistivity (31-54 Ω-m) could be attributed to weathered pumice with sand/silt.

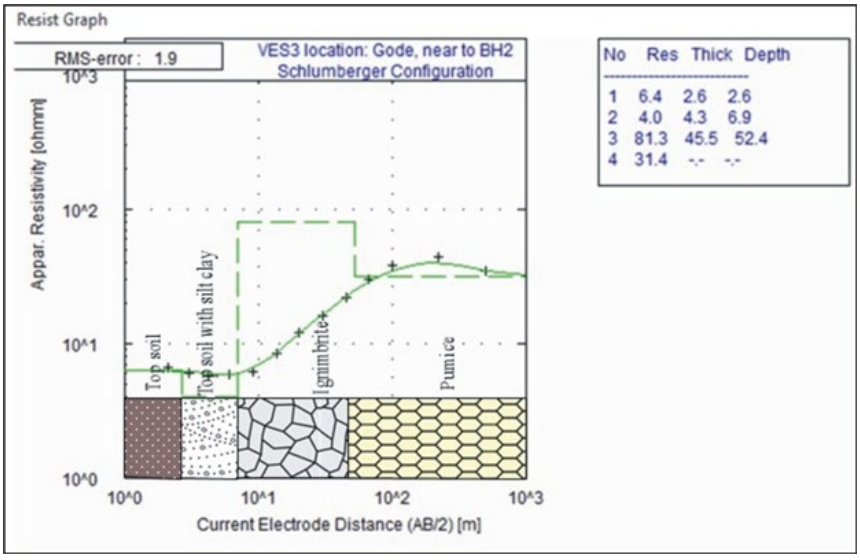

Figure 4. Example of a one-dimensional electrical sounding model and interpreted geological model at VES-3.

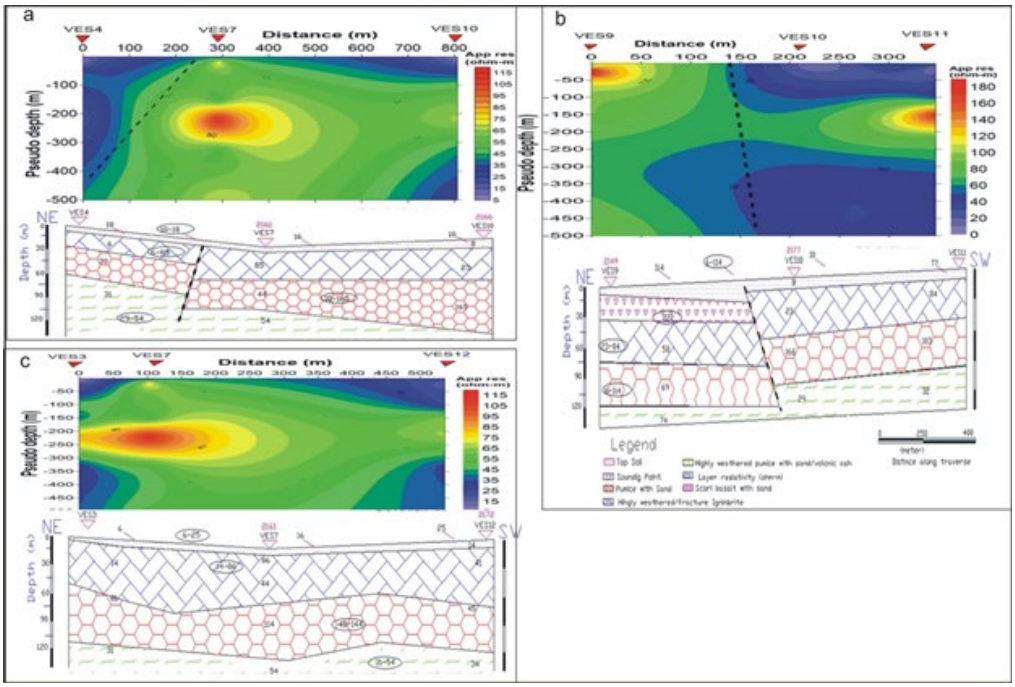

Figure 5. (a-c) Electrical resistivity depth sections (top) constructed from survey lines 1, 5, and 6 (Fig. 3) and geological interpretations (bottom).

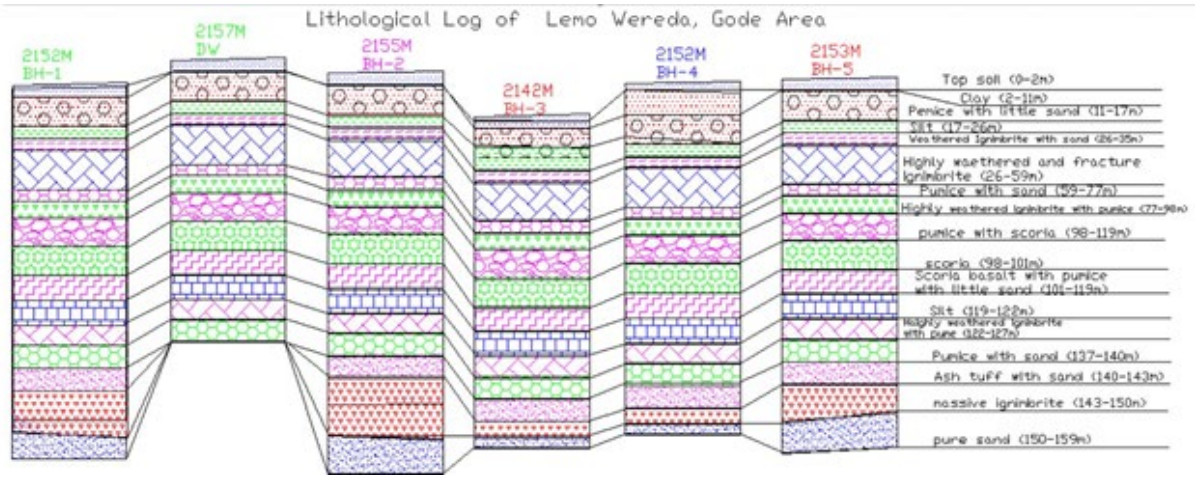

Figure 6. Geological interpretations of the boreholes (Fig. 3).

5. Magnetic Data Interpretation

5.1 Total Magnetic Field Intensity Map

The plot (Fig. 8) illustrates the typical reduction in energy with the increased wavelength, which shows the deep source of (regional anomaly) mean average depth at about 5km and the shallow source of (residual anomaly) mean average depth detected up to 500m of the study area. The prominent geological features observed in the residual magnetic anomaly map are generally preserved in the total and regional magnetic anomaly maps (Fig. 8). A high-pass filter is used to obtain the residual anomaly. The high magnetic susceptibility sediments are derived from the neighboring volcanic rocks. Field observations indicate that the observed residual magnetic anomalies are also governed by the distribution of geologic materials and structural features (Fig. 8). Areas covered by scoriaceous basalt and/or massive ignimbrites are associated with positive magnetic anomalies. The obtained RTP anomalies (Fig. 8) were shifted south and northwards, with the same general trend as the residual anomaly map, but with clear shapes and well-separation from their background. Their overall amplitudes were increased (Figure 9d).

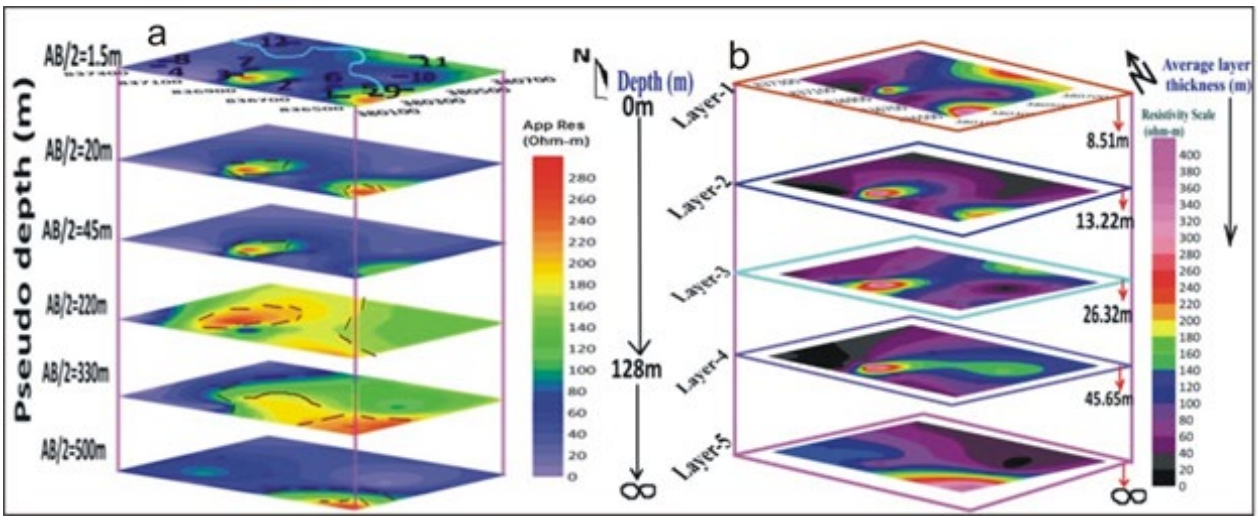

Figure 7. (a) Slices of the electrical resistivity values for different AB/2 distances, and (b) Iso-resistivity depth maps of the subsurface layers.

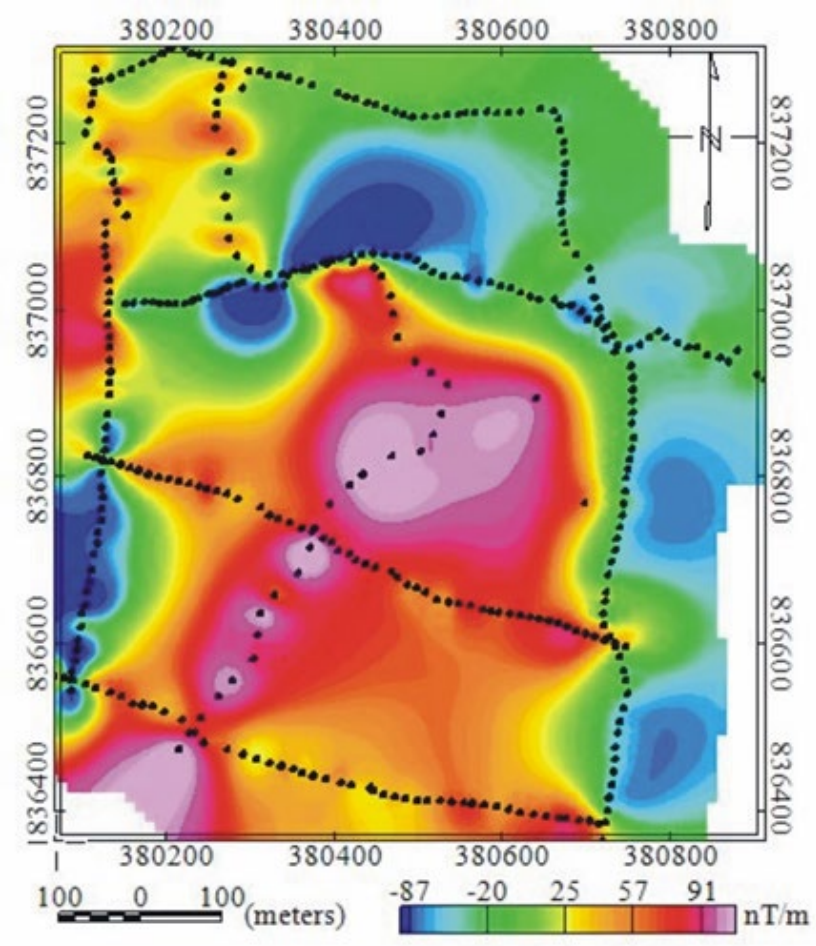

Figure 8. Total magnetic field anomaly map of the study area. Black dots are the location of the magnetic data.

A high-pass filter is used to obtain the residual anomaly. The high magnetic susceptibility sediments are derived from the neighboring volcanic rocks. Field observations indicate that the observed residual magnetic anomalies are also governed by the distribution of geologic materials and structural features (Fig. 8). Areas covered by scoriaceous basalt and/or massive ignimbrites are associated with positive magnetic anomalies. The obtained RTP anomalies (Fig. 8) were shifted south and northwards, with the same general trend as the residual anomaly map, but with clear shapes and well-separation from their background. Their overall amplitudes were increased. The result and discussion part can be summarized in (Table 1a and b).

5.2 Data Enhancement

Derivative methods have been commonly used to interpret gravity and magnetic data to infer the location of lateral boundaries of magnetic susceptibility sources [19, 20]. Several of the derivative methods (e.g., horizontal and vertical derivatives) can produce a series of lineaments from both shallow and deep sources, making the interpretation difficult [21]. To overcome this problem, the tilt derivative method was developed, which uses the ratio of vertical to horizontal derivative and does not have the above problem [20]. The tilt derivative produces tilt angles where a positive tilt angle represents tilt variations within a magnetic susceptibility source, negative values are tilt variations outside a source and zero values represent the edges of a magnetic susceptibility source [20]. Additionally, the analytic signal method [22] was used to compare the results obtained from the tilt derivative analysis. As shown Figure 9d power spectra of the total magnetic data with the linear segments being used to estimate the depth of magnetic susceptibility sources with the lower panel indicating the deeper sources (regional) and shallow sources (residual).

5.2.1 Tilt derivative magnetic map

The tilt derivative or angle map (Fig. 9b) has the attractive property of being positive over magnetic sources, crossing through zero at or near the edge of a vertical-sided source, and is negative outside the source region (Miller and Singh, 1994). Figure 10b is characterized by numerous structures/contacts oriented in the NE-SW and NW-SE directions that are shown by the white solid, dashed lines represent the possible lithological weak zones or fractures.

5.2.2. Euler deconvolution magnetic map

The Euler deconvolution technique is a total derivative method (Miller and Singh, 1994) that can be to the total magnetic anomaly to estimate the magnetic sources' depth and location. In the standard Euler, deconvolution process one must assume a source model which is called the structural index (SI). The structural index values 1, 2, and 3 represent geological features of contact, vertical pipe/horizontal cylinder, and sphere, respectively. And we used a SI = 1 for our study area. The map reveals magnetic sources of different depths marked by different colored symbols plotted on the map where the depths range from 150 to 450 meters. These results are along the edges of magnetic sources and mostly linear and whose locations agree with the analytic signal and tilt derivative analysis. The deeper depths and more linear results occur in the southeast portion of the study area. If these lineations are related to fractures or faults, then the southwestern portion of the study may have a higher water-bearing capacity than the northeast portion.

5.3. 2D Magnetic model.

A 2D forward magnetic model was constructed using the GM-SYS modeling software, to estimate the depth, geometry, and magnetic susceptibilities of the subsurface geological units. .the magnetic model is non-unique, as multiple combinations of magnetic susceptibilities, body geometries, and depths may produce the same magnetic response. To reduce the non-uniqueness, the magnetic model was constructed using depth constraints of a VES profile of VES-4, VES-7, VES-10, and VES-12 (Fig. 3). Figure 10 shows the final magnetic model shows the existence of a weak zone (fracture/fault) below a depth of 25m that extends to 230m depth. A lithologic unit that is described in the model includes; soil ignimbrite, pumice, volcanic ash, and the underlying scoriaceous basalt. The geoelectric section along this profile (Fig. 6a) has the same lithologic units and geological structures except for a slight variation in thickness. Based on the geoelectric section and lithologic log of the borehole, ignimbrite, pumice, and basalt vary in their degree of weathering and fracture. The groundwater system of the area is controlled by highly weathered and fractured horizons and geological structures the possible place to drill for water is shown by the vertical thick yellow line (Fig. 10).

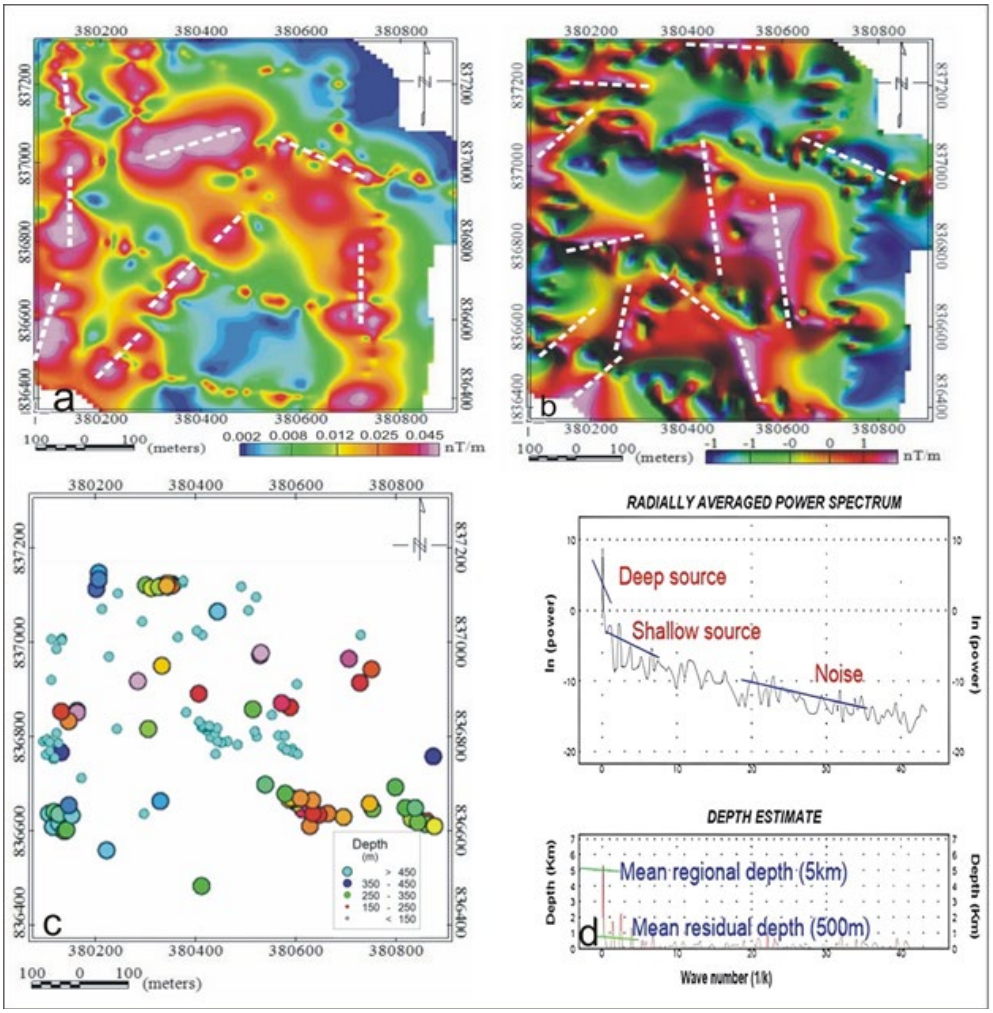

Figure 9. (a) Analytic signal magnetic map of the study area, (b) Tilt derivative of the magnetic map of the study area, and (c) Euler deconvolution depths using the total field magnetic data (Figure 7) of the study area. (d) Power spectra of the total magnetic data with the linear segments being used to estimate the depth of magnetic susceptibility sources with the lower panel indicating the deeper sources (regional) and shallow sources (residual)).

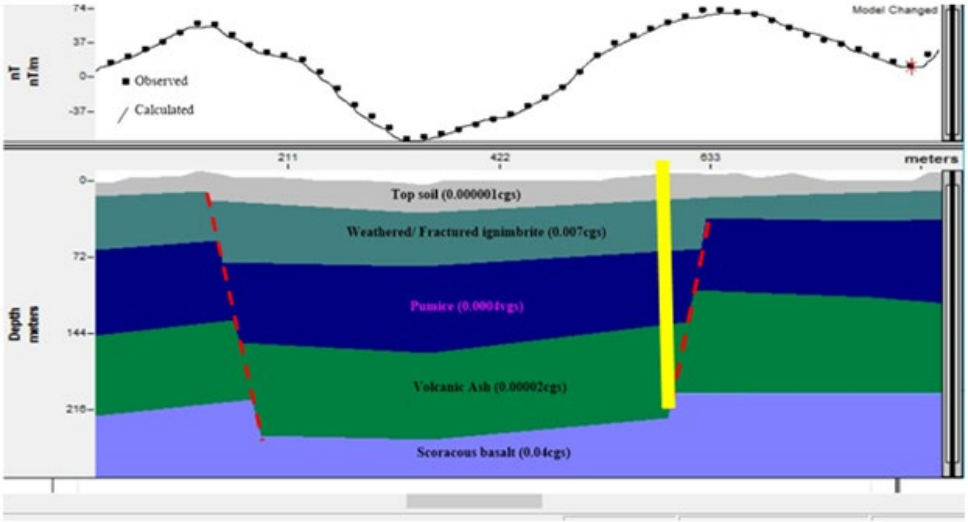

Figure 10. Two-dimensional magnetic model of Line-6 (Fig. 4)

No	Geophysical Methods	Discussion and Analysis
	Electrical Analysis	Magnetic analysis
1	Vertical Electrical Sounding (VES) Analysis	VES- 2, VES- 3, VES-10, and VES-11 are shows good water-bearing zones
2	Pseudo-depth Analysis	Northeast portion of the study area shows unconfined aquifer whereas, southeastern portion shows confined aquifer
3	Iso-resistivity Analysis	The northeast and southeastern portion of the study area shows a low resistivity
4	Geo-electric Analysis	A possible structure/contact zone is depicted in the third and fourth layer of the study area
5	Two-dimensional magnetic Analysis	normal and escarpment faults below a depth of 25 m that extends to 230 m along the survey lines

Table 1 a): Discussion and Analysis

Interpretation Methods	Interpretation Techniques	Results
	VES curve	The vast region under the area shows extensive coverage of the low resistivity zone
Electrical Method Result	Pseudo-depth section	Highly weathered/ fractured pumice/ volcanic ash beneath VES-3, VES-4, VES-7, VES-9, VES-10, and VES-11
	Iso-resistivity	The northeast and southeastern portion of the layer shows a low resistivity region
	Geoelectric section	The third and fourth geoelectric horizons have a large lateral variation in resistivity
	Slice stacked	The northwestern end (unconfined aquifer) or the southeastern part (possibly confined aquifer) of the area.
Magnetic Method Result	Magnetic analytical signal	Result from vertical and horizontal variations/ contacts of geologic structures.
	Total magnetic field intensity	Fresh ignimbrites/ scoriaceous basalt found at a relatively shallower depth, towards the northeast part of Guder River
	Euler deconvolution	The existence of structures (weak zones) that contain highly magnetized bodies in the southeast flank of the current study area.
	Tilt derivative of magnetic	The study area is characterized by numerous structures/contacts oriented in the NE-SW and NW-SE directions
	2D modeling of magnetic	The model reflects existence of a weak zone (fracture/ fault) below a depth of 25m that extends to 230m depth.

Table 1 b): result and Interpretation

6. Conclusions

Vertical electrical sounding (VES) and magnetic survey data collected over several selected profiles and at random points (for the magnetic) have been used to investigate groundwater potential along the Guder River in the Gode area, just northeast of Hosanna town. A total of 12 VES points along six traverses with maximum half-current electrode spacing (AB/2) of 500m have been conducted. Magnetic data of about 405 reading points are also collected systematically along seven profiles that run over the six resistivities (VES) traverses and over random points designed to cover the study area as much as possible. The magnetic data were collected at 10 m station spacing for those conducted on the VES survey lines and about 20 m for the random points. The apparent resistivity pseudo-depth section, sliced-stacked map,

and geoelectric sections show the presence of low resistivity horizons at different depths with their physical suitability to act as aquifer beds. The area's aquifer thickness is obtained from 45m to 92m. The study result revealed that highly weathered and fractured ignimbrite/ pumice with sandy soil is the main water-bearing horizon, which has good groundwater potential, especially between VES-10 and VES-11. Sliced-stacked section constructed from VES data showed the presence of highly conductive horizons (saturated zone), specifically in the eastern direction of the study area.

As shown in the geoelectric sections and 2D magnetic profile plots, the area is transected by several subsurface geological structures (discontinuities), especially in the northeast and southwest part of the area which is important for groundwater flow and occurrence. The 2D magnetic model reflects the existence of normal and escarpment faults below a depth of 25m that extends to 230m along the survey lines VES-4, VES-7, VES-11, VES-10, and VES-12 [23-26].

Acknowledgment

The authors would like to thank the School of Earth Sciences, Addis Ababa University for financial support to conduct this research. We would like to acknowledge Professor Tigistu Haile for his invaluable assistance during the study and constructive guidance in all aspects of this research. We would also like to thank anonymous reviewers for their valuable comments and suggestions.

References

1. Berhane, G., Kebede, S., Gebreyohannes, T., Martens, K., Van Camp, M., & Walraevens, K. (2016). An integrated approach for detection and delineation of leakage path from Micro-Dam Reservoir (MDR): a case study from Arato MDR, Northern Ethiopia. Bulletin of Engineering Geology and the Environment, 75, 193-210.
2. Farrag, A. A., Ebraheem, M. O., Sawires, R., Ibrahim, H. A., & Khalil, A. L. (2019). Petrophysical and aquifer parameters estimation using geophysical well logging and hydrogeological data, Wadi El-Assiuoti, Eastern Desert, Egypt. Journal of African Earth Sciences, 149, 42-54.
3. Shishaye, H. A., & Abdi, S. (2016). Groundwater exploration for water well site locations using geophysical survey methods. Hydrol. Curr. Res, 7(1).
4. Ayenew, T., Demlie, M., & Wohnlich, S. (2008). Hydrogeological framework and occurrence of groundwater in the Ethiopian aquifers. Journal of African Earth Sciences, 52(3), 97-113.
5. Farrag, A. A., Riad, S., & Ahmed, M. H. (2002). Groundwater situation and evaluation in the Nile Basin East of Assiut, Egypt. J Eng Sci Assiut Univ, 30(2), 517-542.
6. Yousef, A. F. (2008). The Impact of North West Active Fault System on the Recharge of the Quaternary Aquifer System around the Nile Valley: Case Study Wadi El-Assiuty, Eastern Desert. Egypt. European Water, 21(22), 41-55.
7. Ali, H. Y., Priju, C. P., & Prasad, N. N. (2015). Delineation of groundwater potential zones in deep midland aquifers along Bharathapuzha river basin, Kerala using geophysical methods. Aquatic Procedia, 4, 1039-1046.
8. Araffa, S. A. S., Mohamed, A. M., & Santos, F. M. (2017). Geophysical investigation in the Northwestern part of the Gulf of Suez, Egypt. Egyptian journal of petroleum, 26(2), 457-475.
9. Dereje, B., & Nedaw, D. (2019). Groundwater recharge estimation using WetSpass modeling in Upper Bilate Catchment, southern Ethiopia. Momona Ethiopian Journal of Science, 11(1), 37-51.
10. Araffa, S. A., Mohamadin, M. I., Saleh Sabet, H., & Takey, M. S. (2019). Geophysical interpretation for groundwater exploration around Hurghada area, Egypt. NRIAG Journal of Astronomy and Geophysics, 8(1), 171-179.
11. Araffa, S. A. S. (2013). Delineation of groundwater aquifer and subsurface structures on North Cairo, Egypt, using integrated interpretation of magnetic, gravity, geoelectrical and geochemical data. Geophysical Journal International, 192(1), 94-112.
12. Ebinger, C. (2005). Continental break-up: the East African perspective. Astronomy & Geophysics, 46(2), 2-16.
13. Woldegabriel, G., Aronson, J. L., & Walter, R. C. (1990). Geology, geochronology, and rift basin development in the central sector of the Main Ethiopia Rift. Geological Society of America Bulletin, 102(4), 439-458.
14. Flathe, H. (1955). Possibilities and limitations in applying geoelectrical methods to hydrogeological problems in the coastal areas of north west Germany. Geophysical prospecting, 3(2), 95-109.
15. Flathe, H. (1970). Interpretation of geoelectrical resistivity measurements for solving hydrogeological problems. Minning and Groundwater Geophysics: Geological Survey of Canada. Economic Geological Report, 26, 580-597.
16. Zohdy, A. A., Eaton, G. P., & Mabey, D. R. (1974). Application of surface geophysics to ground-water investigations (No. 02-D1). US Dept. of the Interior, Geological Survey: US Govt. Print. Off.,.
17. Telford, W. M., Geldart, L. P., & Sheriff, R. E. (1990). Applied geophysics. Cambridge university press.
18. Kearey, P., Brooks, M., & Hill, I. (2002). An introduction to geophysical exploration (3rd). Great Britain: Blackwell Science Ltd.
19. Cordell, L. (1979). Gravimetric expression of graben faulting in Santa Fe country and the Espanola basin, New Mexico. In Guidebook to Santa Fe Country, 30th Field Conference, 1979 (pp. 59-64). New Mexico Geological Survey.
20. Salem, A., Williams, S., Fairhead, D., Smith, R., & Ravat, D. (2008). Interpretation of magnetic data using tilt-angle derivatives. Geophysics, 73(1), L1-L10.
21. Demissie, Z., Mickus, K., Bridges, D., Abdelsalam, M. G., & Atekwana, E. (2018). Upper lithospheric structure of the Dobi graben, Afar Depression from magnetics and gravity data.

Journal of African Earth Sciences, 147, 136-151.
22. Dentith, M., & Mudge, S. T. (2014). Geophysics for the mineral exploration geoscientist. Cambridge University Press.
23. Ishola, K., Ogunsanya, S., Adiat, K., & Abdulrahman, A. (2013). Assessing groundwater potential zones in basement complex terrain using resistivity depth soundings: a case of challenge and Oluyole in Ibadan, Southwestern. Nigeria Journal of Science, 1(1), 11-32.
24. Henriet, J. P. (1976). Direct applications of the Dar Zarrouk parameters in ground water surveys. Geophysical prospecting, 24(2), 344-353.
25. Dar, I. A., Sankar, K., & Dar, M. A. (2010). Remote sensing technology and geographic information system modeling: an integrated approach towards the mapping of groundwater potential zones in Hardrock terrain, Mamundiyar basin. Journal of Hydrology, 394(3-4), 285-295.
26. Maillet, R. (1947). The fundamental equations of electrical prospecting. Geophysics, 12(4), 529-556.

Copyright: *©2023 Esubalew Yehualaw Melaku, et al. This is an open-access article distributed under the terms of the Creative Commons Attribution License, which permits unrestricted use, distribution, and reproduction in any medium, provided the original author and source are credited.*